

Analysis and application of automatic deformation monitoring data for buildings and structures of mining area

XIAO Jie^{1,2,3}, ZHANG Jin⁴

1. Institute of Geodesy and Geophysics, Chinese Academy of Sciences, Wuhan 430077, China;
2. Key Laboratory of Dynamic Geodesy, Institute of Geodesy and Geophysics, Chinese Academy of Sciences, Wuhan 430077, China
3. Graduate School of Chinese Academy of Sciences, Beijing 100049, China;
4. Department of Surveying and Mapping, Taiyuan University of Technology, Taiyuan 030024, China

Received 19 June 2011; accepted 10 November 2011

Abstract: The buildings and structures of mines were monitored automatically using modern surveying technology. Through the analysis of the monitoring data, the deformation characteristics were found out from three aspects containing points, lines and regions, which play an important role in understanding the stable state of buildings and structures. The stability and deformation of monitoring points were analysed, and time-series data of monitoring points were denoised with wavelet analysis and Kalman filtering, and exponent function and periodic function were used to get the ideal deformation trend model of monitoring points. Through calculating the monitoring data obtained, analyzing the deformation trend, and cognizing the deformation regularity, it can better service mine safety production and decision-making.

Key words: wavelet analysis; Kalman filtering; deformation monitoring data analysis; mine

1 Introduction

Mine ground hazards seriously affect the safe production of mine, and the deformation state of buildings and structures built on the soft ground in mines is directly related to the safety of mines production facilities. The buildings and structures of mines are monitored automatically using modern surveying technology. In order to find out the stable state of buildings and structures timely and effectively, the deformation characteristics were analyzed from three aspects contained points, lines and regions using the deformation monitoring data, also the deformation trends and regularity were cognized, which can better service mine safety production and decision-making.

There are two main methods, including routine analysis and mathematical model analysis, to analyze the deformation monitoring data and describe the deformation states. The method of routine analysis can cognize the stability of the buildings and structures by calculating the tilt, rotation, twist, bend and so on with the coordinates of monitoring points [1–2], or understand

the deformation trends in the ways such as construction and comparison methods. Mathematical model analysis methods usually contain statistical analysis, time series analysis, grey theory and so on [3–5]. As deformation monitoring data are inevitably subjected to a variety of noise interference, the observed data are usually contaminated. In order to improve the accuracy and reliability of monitoring data, the error analysis of deformation data sequence is required first of all. The methods of wavelet analysis [6–10] and Kalman filtering, which have a high application value in engineering practice, respectively [11–12], were widely used at home and abroad to reduce the noise. In this work, the actually measured deformation data are analyzed, with mathematical statistics, wavelet analysis and Kalman filtering method to denoise monitoring data sequence to obtain deformation trends of monitoring points.

2 Fundamental analysis for deformation of monitoring points

In a large open-air coal production base, due to the trestle of washery building on the backfill soft ground,

part of the supporting pillars and trestles have deformed. So, some of dangerous buildings and structures of mining area were monitored using integrated automatic deformation monitoring system combined with GPS and TPS [13]. The area includes 15 groups of supporting pillars groups of the trestle, which can be divided into two kinds of cases, i.e. four pillars group and two pillars group.

In order to monitor the subsiding and tilt of supporting pillars, the prisms were mounted on the pillars. The instrument is high precision TPS, and 51 prisms were mounted on the pillars. The coordinates of instrument station and target point were updated by the results of 24 h GPS post-processing solution. The monitoring lasted intermittently for 389 d from August 23, 2008 to September 16, 2009, and 51 periods monitoring data were obtained.

In the horizontal direction, the pillar groups 1–12 were moving to the southeast, and the other pillar groups were moving to the northwest. The offset of pillar group 12 was the minimum in the horizontal direction, and the deformation region can be divided into two subregions by the pillar group 12. In the vertical direction, the group with the most obvious subsidence is pillar group 5. The minimum subsidence is -0.267 m, and the maximum subsidence is up to -0.281 m. The groups with the second larger subsidence are the pillar groups 1–4. The maximum subsidence is -0.194 m, and the minimum subsidence is -0.155 m. And other pillar groups have the relatively smallest subsidence. The maximum subsidence is -0.119 m, and the minimum subsidence is -0.062 m. The accumulated deformation trends for all 51 monitoring points are shown in Fig. 1.

According to the further investigation of the trestle foundation, the surrounding around the sites as well as the analysis of the monitoring data, the main reasons giving rise to the deformation of the monitoring point are concluded as follows.

1) The foundation factor. The type of the structure foundation is soft ground of backfill with obvious rheological effect, where the main ingredient is rock composed of clay mineral. Such type of ground with a tendency to be porous not only has a strong expansion, but also loses its strength after immersion with water, which can cause the move of the pillars, such as pillar groups 8 and 9. In addition, the different depth of ground will lead to different carrying capacity with the same load, which will induce uneven subsidence of pillar groups, especially in the case of stacking heavy machinery around the pillars for long time, which induces overload damage and makes the ground subsidence. When the weight of stacking loads on both sides around the pillar is seriously uneven, it may cause the ground tilt, leading to uneven subsidence of the

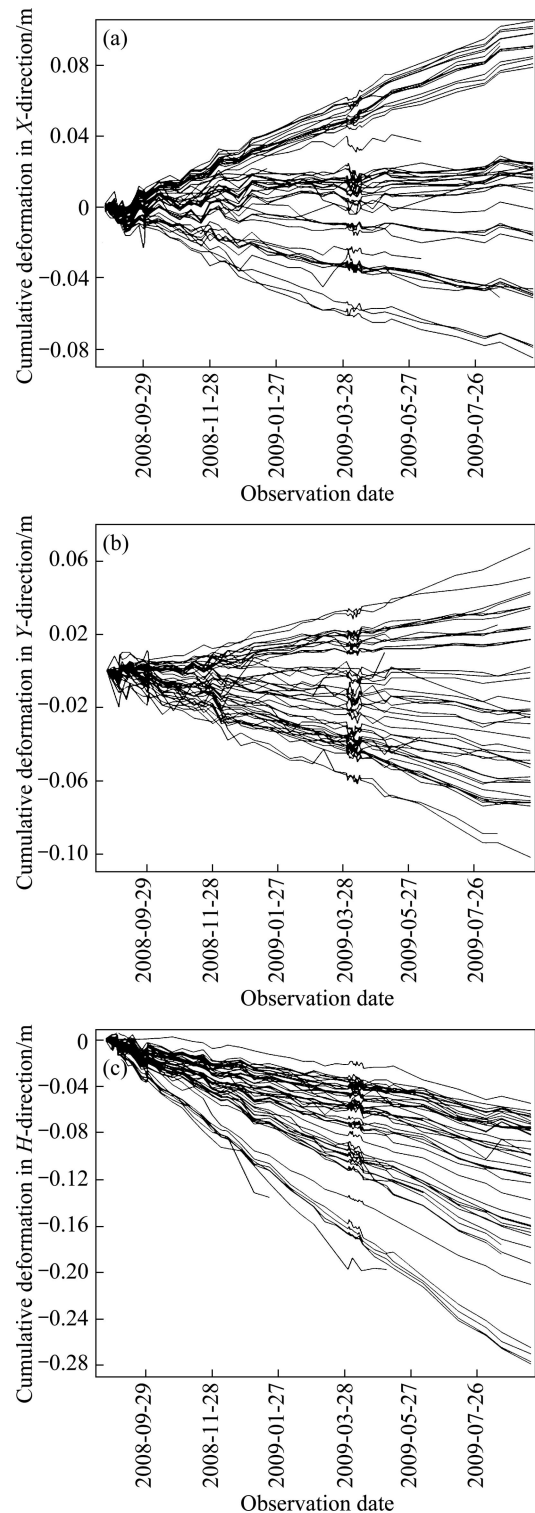


Fig. 1 Cumulative deformation for all monitoring points

pillars. It can be seen that the reason of subsidence of pillar group 5 is that the ground around the pillars has been extruded for a long time by large number of heavy machinery and vehicles, also the weights of loads on both sides of the pillars are severely uneven, which causes the ground tilt. And all these reasons make the ground sink, and so the deformation of the monitoring points of the region is the largest.

2) Load impact. A long-term coal transportation, the weight of the trestle itself supported by pillars, and the extrusion of the coal pile to the pillars, will all lead to the displacement of the pillars.

3) Different materials and structures of pillar impact. The steel pillar group 1 is prone to be affected by the atmospheric temperature, humidity and so on, which will result in thermal expansion and contraction and the monitoring points displacement. The slight deformation often takes on circle regularity with the seasonal variation. In addition, the long-term trestle force will make the pillars bend. From the figures, it can be seen obviously that the deformation of the group 1 is larger than those of other pillar groups constructed of reinforced concrete.

3 Signal denoising to deformation data of monitoring points

Deformation data affected by several factors are nonstationary time series, which are function of time. The data wave randomly near the tendency of the curve in the time course of the time series. The tendency of the curve may be a linear function, power function or exponential function, which may be stable growth or attenuation. It also may be sine or cosine function which waves up and down along with the time cycle, or superposition of several curves. Usually deformation data are considered to be the superposition of the deformation information item and noise interference items. Therefore, the deformation data got by observation are not real deformation. Deformation information items can be divided into trend and periodic terms and other information. The movement of the trend item is in a particular direction, the deformation of which is due to the changes of the surrounding environment and the structures affected by the long-term loads and the influence of natural factors. The periodic term is periodic information recognized according to the observation frequency, which is due to the cyclical changes of temperature and season. Noise item is caused by instability of the observational instruments and random factors. It is necessary to denoise monitoring data before analyzing the deformation of the structure.

3.1 Wavelet denoising

Wavelet analysis is a time-frequency analysis method with characteristics of multi-resolution analysis, which is a time-frequent localizing analysis method whose window size is fixed but the window shape, time window and frequency window can be changed. Deformation data sequence will be processed as a time-frequency signal. The original deformation data are viewed as the superposition of the deformation

information and noise signals, the representation is as follows,

$$f(i) = s(i) + n(i) \quad (1)$$

where $s(i)$ is the true deformation signal; $n(i)$ is Gaussian white noise as $n(i) \in N(0, \sigma^2)$. The time-frequent properties of deformation signal and noise signal are usually different with the deformation data sequence. In the time-frequency domain, the deformation signal is low-frequency localization, while the noise signal is high-frequency signal, which is the global distribution. Denoising method using wavelet analysis is essentially wavelet transformation in different scales, and filtering the signal using band-pass filter with different center frequencies, separating the high-frequency signal and the low-frequency effectively to achieve the purpose of denoising. About the selection of maximum scale J using wavelet transformation, the problem is resolved by increasing the scale gradually in this work. Then scale J is determined based on whether the change of the root mean square error (E_{RMS}) tends to stability or not.

When the maximum scale J is taken as $k=1, 2, 3, \dots$, E_{RMS} is calculated respectively.

$$r_{k+1} = \frac{E_{\text{RMS}}(k+1)}{E_{\text{RMS}}(k)} \quad (k = 1, 2, 3, \dots, L) \quad (1)$$

where r is the ratio of two E_{RMS} values when k takes different values. When the r value gets closer to 1, the effect of denoising will be better [14].

During the data processing for deformation monitoring, Daubechies wavelets are widely used, also known as DbN wavelet, which is an orthogonal and compactly supported wavelet. With the increase of N , the regularity of Daubechies wavelets will be better, that is the better smoothness. The data sequence of the point X2Z13QS in the vertical direction was taken as an example for wavelet decomposition and reconstruction using the Db2 and Db6 filters. When it is taken with different scales, the calculated results of the estimated E_{RMS} between the original signal and denoised signal is listed in Table 1. From Table 1 it can be seen that the effect of denoising effect is better when using Db6 filter and taking maximum scale $J=2$.

Table 1 Root mean square error of wavelet decomposition and reconstruction filter method in different scales

Maximum scale J	E_{RMS}/m		r_k	
	Filter(Db2)	Filter(Db6)	Filter(Db2)	Filter(Db6)
$K=1$	0.001 6	0.001 7	–	–
$K=2$	0.001 9	0.002 0	1.19	1.18
$K=3$	0.002 5	0.003 1	1.32	1.55
$K=4$	0.003 0	0.003 6	1.20	1.16

Figure 2 shows the two layers detail signals of Db6 wavelet decomposition in the vertical direction for monitoring point (X2Z13QS). From Fig. 2, it can be seen that the curve is smooth after denoising, and the noise is removed well. According to the noise signal to be filtered, the size of the noise can be evaluated, then the observed error values can be estimated.

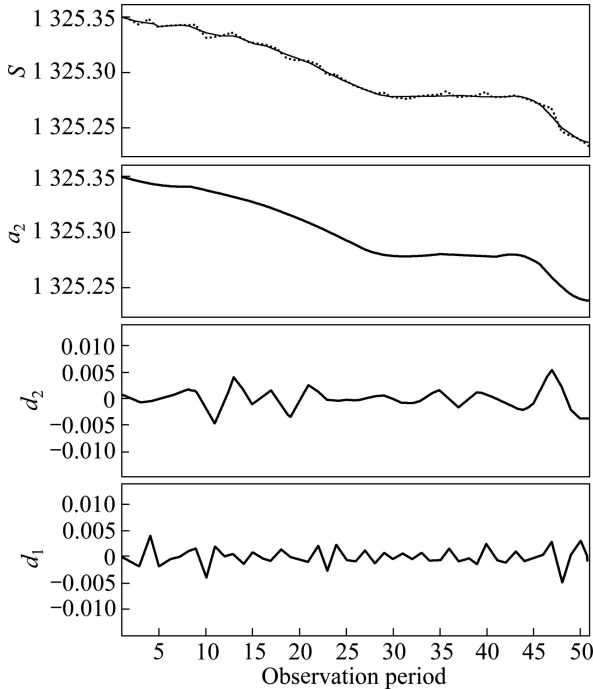


Fig. 2 Two layers detail signals of Db6 wavelet decomposition in vertical direction for monitoring point (X2Z13QS)

3.2 Kalman filtering denoising

Kalman filtering method is nowadays most widely used as a dynamic data processing method, with the minimum unbiased variance and significantly improving the precision of dynamic positioning, and its greatest feature is the ability to eliminate random interference noise to obtain useful information, which is approximately the true situation [15]. Through the recursive way and by the help of state transition matrix and observation data of the system itself, Kalman filtering method optimally estimates the system state to predict the system state of the future in real time. Deformation monitoring data observed are discrete. Therefore, the discrete Kalman filter model equation is

$$\begin{cases} \mathbf{X}_k = \Phi_{k,k-1}\mathbf{X}_{k-1} + \Gamma_{k,k-1}\boldsymbol{\Omega}_{k-1} \\ \mathbf{Z}_k = \mathbf{H}_k\mathbf{X}_k + \Delta_k \end{cases} \quad (2)$$

where \mathbf{X}_k is the system state vector at the moment t_k , $\Phi_{k,k-1}$ is the system state transition matrix from the moment t_{k-1} to t_k , $\boldsymbol{\Omega}_{k-1}$ is the system state noise at the moment t_{k-1} ; $\Gamma_{k,k-1}$ is the noise input matrix at the moment t_k ; \mathbf{Z}_k is the system observation vector at the

moment t_k ; \mathbf{H}_k is the system measurement matrix at the moment t_k ; and Δ_k is the system measurement noise at the moment t_k .

The deformation speed of the monitoring points is usually slow in deformation monitoring of the structures. So three-dimensional displacement and speed can be expressed as the system state vector $\mathbf{X}(t)$, while the three-dimensional acceleration can be expressed as the system state noise vector $\boldsymbol{\omega}(t)$. The system state equation is

$$\begin{bmatrix} \mathbf{x}(t) \\ \mathbf{y}(t) \\ \mathbf{h}(t) \\ \mathbf{v}_x(t) \\ \mathbf{v}_y(t) \\ \mathbf{v}_h(t) \end{bmatrix}_k = \begin{bmatrix} 1 & 0 & 0 & \Delta t_k & 0 & 0 \\ 0 & 1 & 0 & 0 & \Delta t_k & 0 \\ 0 & 0 & 1 & 0 & 0 & \Delta t_k \\ 0 & 0 & 0 & 1 & 0 & 0 \\ 0 & 0 & 0 & 0 & 1 & 0 \\ 0 & 0 & 0 & 0 & 0 & 1 \end{bmatrix}_{k,k-1} \begin{bmatrix} \mathbf{x}(t) \\ \mathbf{y}(t) \\ \mathbf{h}(t) \\ \mathbf{v}_x(t) \\ \mathbf{v}_y(t) \\ \mathbf{v}_h(t) \end{bmatrix}_{k-1} + \begin{bmatrix} \frac{1}{2}\Delta t_k^2 & 0 & 0 \\ 0 & \frac{1}{2}\Delta t_k^2 & 0 \\ 0 & 0 & \frac{1}{2}\Delta t_k^2 \\ 1 & 0 & 0 \\ 0 & 1 & 0 \\ 0 & 0 & 1 \end{bmatrix}_{k,k-1} \begin{bmatrix} \boldsymbol{\omega}_x(t) \\ \boldsymbol{\omega}_y(t) \\ \boldsymbol{\omega}_h(t) \end{bmatrix}_{k-1} \quad (3)$$

The observation equation is

$$\begin{bmatrix} \mathbf{x}(t) \\ \mathbf{y}(t) \\ \mathbf{h}(t) \\ \mathbf{v}_x(t) \\ \mathbf{v}_y(t) \\ \mathbf{v}_h(t) \end{bmatrix}_k = \begin{bmatrix} 1 & 0 & 0 & 0 & 0 & 0 \\ 0 & 1 & 0 & 0 & 0 & 0 \\ 0 & 0 & 1 & 0 & 0 & 0 \end{bmatrix}_{k,k-1} \begin{bmatrix} \mathbf{x}(t) \\ \mathbf{y}(t) \\ \mathbf{h}(t) \\ \mathbf{v}_x(t) \\ \mathbf{v}_y(t) \\ \mathbf{v}_h(t) \end{bmatrix}_{k-1} + \begin{bmatrix} \Delta_x(t) \\ \Delta_y(t) \\ \Delta_h(t) \end{bmatrix}_{k-1} \quad (2)$$

In the next, the data sequence of point (X2Z13QS) in the vertical direction is taken as an example. Using Kalman filtering method to denoise the data, the results in the Fig. 3 show that Kalman filtering method reflects the actual situation well, and the root mean square error (E_{RMS}) is 0.002 2 m. Figure 4 shows the comparative results of Kalman filtering and wavelet analysis methods.

It can be seen from Fig.4 that the denoising effect has great consistency, and the both two methods obtain satisfactory results.

4 Analysis of deformation trends fitting

During the deformation monitoring, it is impossible to take into account all the reasons causing deformation

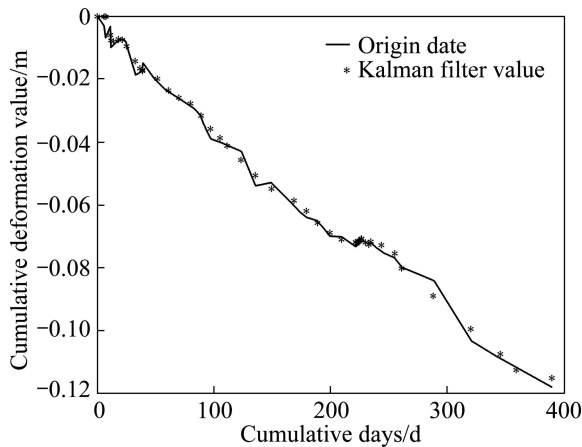


Fig. 3 Denoising result of Kalman filtering

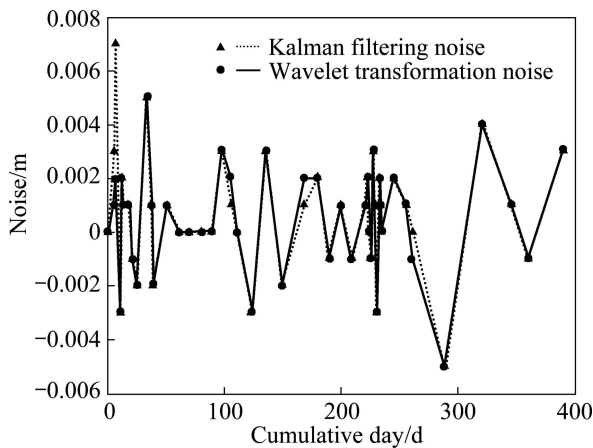


Fig. 4 Comparison results of Kalman filtering and wavelet analysis

and parameterize them. Therefore, it often extract the deformation trend by fitting method. Usually, for some points with simple movement patterns, polynomial fitting can be used to achieve very good results. For the points with the relatively complex movement patterns, the combination way of several models can be chosen for fitting. The following are several forms commonly used in the combination model.

1) Polynomial fitting. In the fitting model, using piecewise polynomial to approximate any continuous function is the simplest case, and the polynomial model is as follows:

$$x_t = a_0 + \sum_{k=1}^n A_k t^k + \varepsilon_t \tag{3}$$

2) Exponent trends. Sometimes the data series show the exponential growth or decay trend. The model is as follows:

$$x_t = \sum_{k=1}^n A_k e^{a_k t} + \varepsilon_t \tag{4}$$

3) Periodic trends. If the data sequence shows a regular cyclical up and down, and the following fitting model can be used:

$$x_t = C_k \sin(k\omega t) + D_k \cos(k\omega t) + \omega_t \tag{5}$$

The three combinations in fitting models are commonly used, and when dealing with specific issues, it is necessary to determine the fitting model according to their physical background and specific analysis of the observed data. During the polynomial fitting methods, the k value is given, such as $k=1, 2, 3, \dots$, that is the order is increased gradually. When the order is added each time, the fitting coefficients and fitting values will be calculated, and the residual sum of squares will also be calculated. F test is used between two fitting, and with the increase of the order, the residual sum of squares is not decreased significantly, indicating that the order of fitting has reached the best fit number.

The vertical direction of monitoring point (X2Z13QS) is taken as an example. Firstly, the monitoring data after denoising are used to calculate the accumulated deformation, and then the exponential model is used for fitting. The fitting results are shown in Fig. 5. Figure 5(a) shows the fitting result of the exponential, Fig. 5(b) shows the fitting of periodic function using the residual items after the exponential fitting, and Fig. 5(c) shows the final residuals. The fitting formula is

$$y_1 = -0.03764e^{0.003014t} + 0.03925e^{-0.01088t} - 0.001189\cos(0.0181t) + 0.000054\cos(0.0181t) + 0.00231\cos(0.0362t) - 0.00079\sin(0.0362t) + 0.000337$$

Finally, the root mean square error of fitting is equal to 0.001 419, and the fitting results is very ideal.

The Kalman filtering method and the quadratic residuals of unequal interval GM(1,1) model were compared to the same set of data, and the algorithms can be found in Ref. [16–17]. The comparative results are shown in Figs. 6 and 7. It can be seen from the figures that the three methods can achieve qualified fitting prediction results; by contrast, the Kalman filtering method makes the results of predictions have a larger fluctuation due to the few number of observations in the initial stage, but the other two methods have considerable prediction accuracy.

5 Conclusions

1) The noise fluctuations of Kalman filtering method is larger in the initial stage, and the reason is that the number of observations is too few and the initial value setting is not accurate, while the noise size of

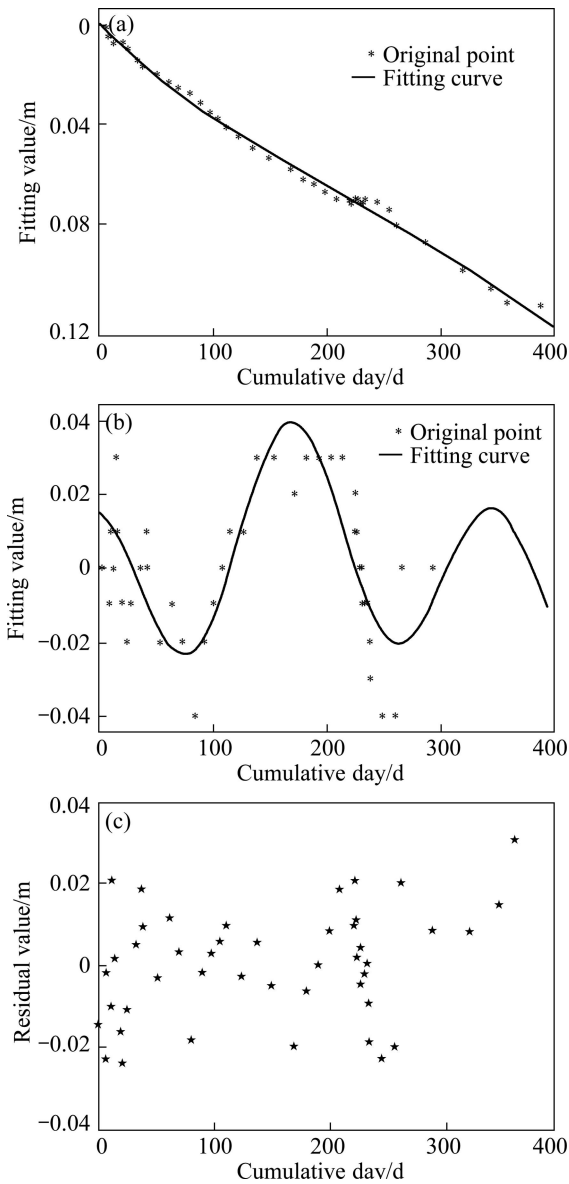


Fig. 5 Fitting curve and residual plots: (a) Plot of exponent function fitting; (b) Plot of periodic function fitting; (c) Residual plot

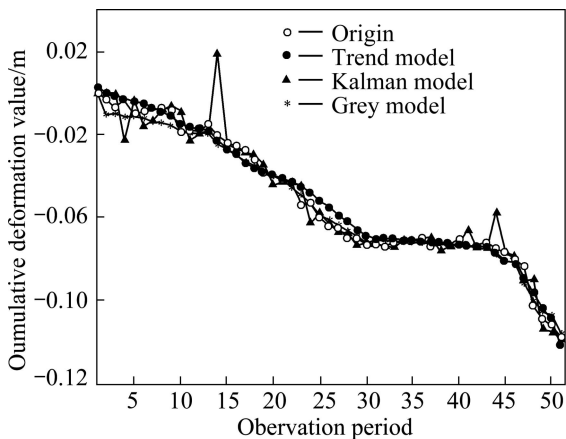


Fig. 6 Comparison of fitting curves of three models

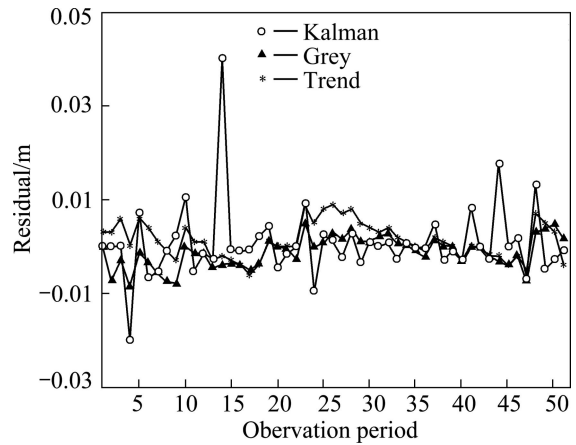


Fig. 7 Fitting residuals of three models

Kalman filtering method keeps pace compared with the result of wavelet denoising method in the later stage.

2) The root mean square error of deformation trends fitting for the monitoring points based on exponential function and periodic function is less than 1.5 mm.

References

- [1] ESRA T E, RAHMI N C, TEVFIK A. Structural deformation monitoring analysis using geodetic techniques after the earthquake at Bolu pass of trans-European motorway [C]//Proceedings of the 13th FIG symposium on deformation measurement and analysis. Lisbon: International Federation of Surveyors (FIG), 2008: 1–9.
- [2] JAN D W, XIAO Y C, PAFFENHOLZ J A. Geodetic monitoring and deformation analysis of a vertical lift bridge [C]//Proceedings of the 13th FIG symposium on deformation measurement and analysis. Munich: International Federation of Surveyors (FIG), 2006: 1–15.
- [3] CHEN Yong-qi, TANG C. Application of the theory of grey theory system in the analysis of the deformation surveying [C]//Proceedings of the 7th International FIG symposium on deformation measurements. Alberta: International Federation of Surveyors (FIG), 1993: 303–309.
- [4] HUANG Ming, GE Xiu-run, WANG Hao. Application of grey model in linear deformation measurement of rock mass [J]. Chinese Journal of Rock Mechanics and Engineering, 2001, 20(2): 235–238. (in Chinese)
- [5] TOR Y K. L1, L2, Kalman Filter and time series analysis in deformation analysis [C]//Proceeding of the FIG XXII International Congress. Washington: International Federation of Surveyors (FIG), 2002: 1–18.
- [6] WU Zhao-fu, GAO Fei, TAO Ting-ye. Application of noise information based on wavelet transformation in evaluating precision of dam deformation monitoring [J]. Advances in Earth Science, 2008, 23(6): 590–594. (in Chinese)
- [7] HUANG Sheng-xiang, LIU Jing-nan. A novel method for reducing noises in GPS deformation monitoring system [J]. Acta Geodaetica et Cartographica Sinica, 2002, 31(2): 104–107. (in Chinese)
- [8] TIAN Sheng-li, ZHOU Yong-jun, GE Xiu-run. Processing of monitoring data of building deformation based on wavelet transform [J]. Chinese Journal of Rock Mechanics and Engineering, 2004,

- 23(15): 2639–2642. (in Chinese)
- [9] WANG Jian, GAO Jing-xiang, ZHENG Nan-shan. Monitoring subsidence time series analysis based on wavelet theory [J]. Journal of Geodesy and Geodynamics, 2005, 25(4): 91–95. (in Chinese)
- [10] HUANG Sheng-xiang, LIU Jing-nan, LIU Xiang-lin. Deformation analysis based on wavelet and its application in dynamic monitoring for high-rise buildings [J]. Acta Geodaetica et Cartographica Sinica, 2005, 32(2): 153–157. (in Chinese)
- [11] TOR Y K. Application of Kalman filter in real-time deformation monitoring using surveying robot [J]. Civil Engineering Research, 2003(16): 92–95.
- [12] MA Pan, MENG Ling-kui, WEN Hong-yan. Kalman filtering model of dynamic deformation based on wavelet analysis [J]. Geomatics and Information Science of Wuhan University, 2004, 29(4): 349–353. (in Chinese)
- [13] GUI Hui-hong, ZHANG Jin, CHEN Yong-jian. Research of Georobot online automatic deformation monitoring software development based on GTS901A [J]. Science of Surveying and Mapping, 2010, 35(4): 166–168. (in Chinese)
- [14] ZHANG Zheng-lu, HUANG Quan-yi, WEN Hong-yan. Analysis and prediction of deformation monitoring in engineering [M]. Beijing: Surveying and Mapping Press, 2007. (in Chinese)
- [15] LIU Hong-xin, WANG Jie-xian, WANG Tian-xiang. Analysis of adaptive Kalman filtering in deformation monitoring of bridges [J]. Journal of Tongji University: Natural Science, 2005, 33(8): 1027–1030. (in Chinese)
- [16] LI Ke-gang, XU Jiang, HUANG Guo-yao. Prediction for slope displacement based on unequal interval GM(1, 1) model [J]. Chinese Journal of Underground Space and Engineering, 2006, 2(6): 988–992. (in Chinese)
- [17] HANG Sheng-xiang, Yin Hui, JIANG Zheng. Deformation monitoring and data processing [M]. Wuhan: Wuhan University Press, 2003. (in Chinese)

(Edited by HE Yun-bin)